Large enhancement in high-energy photoionization of Fe XVII and missing continuum plasma opacity

Sultana N. Nahar* and Anil K. Pradhan†
Department of Astronomy, The Ohio State University, Columbus, Ohio 43210.

Aimed at solving the outstanding problem of solar opacity, and radiation transport plasma models in general, we report substantial photoabsorption in the high-energy regime due to atomic core photo-excitations not heretofore considered. In extensive R-Matrix calculations of unprecedented complexity for an important iron ion Fe XVII (Fe^{16+}), with a wave function expansion of 99 Fe XVIII (Fe^{17+}) LS core states from $n \leq 4$ complexes (equivalent to 218 fine structure levels), we find: i) up to orders of magnitude enhancement in background photoionization cross sections, in addition to strongly peaked photo-excitation-of-core resonances not considered in current opacity models, and ii) demonstrate convergence with respect to successive core excitations. The resulting increase in the monochromatic continuum, and 35% in the Rosseland Mean Opacity, are compared with the "higher-than-predicted" iron opacity measured at the Sandia Z-pinch fusion device at solar interior conditions.

PACS number(s) :32.80.Aa,32.80.Fb,32.80.Zb,95.30.Ky

arXiv:1606.02731v1 [astro-ph.SR] 8 Jun 2016

Radiation transport and light-matter interactions depend fundamentally on plasma opacity, which in turn entails an intricate interplay of atomic and plasma effects under local conditions. In astrophysics, monochromatic and mean opacities, averaged over photon-particle distributions, are crucial to the determination of not only emergent spectra but also the chemical composition of the source. Surprisingly, elemental abundances of the Sun have been called into question in recent years, and revised downwards by up to ∼50% for common elements such as C, N, O and Ne [1]. But that has posed an outstanding problem for stellar interior and helioseismic models [2]. Recent laboratory measurements of monochromatic iron opacity at the Sandia Z-pinch machine of plasma created at conditions similar to those near the convection and radiative zone boundary disagree considerably with current opacity models by 30-400% in the wavelength range of 7-13Å [3]. Discrepancies are evident not only at and between energies where discrete transitions occur but, more surprisingly, the measured opacity is substantially higher in the high-energy featureless bound-free continua (or photoionization) of a few abundant iron ions Fe XVII , Fe XVIII and Fe XIX . The *upward* revision of opacities [3] tends to support the revised *lower* solar abundances. Indeed, the measured Z opacity for iron alone enhances the solar mixture opacity of all abundant elements by ∼7%, about half of the 15% required to reconcile with stellar interior and helioseismic models. We show that hitherto neglected atomic and plasma physics may have a significant bearing on the missing opacity problem.

Current opacity models generally consider photoexcitations into the continuum as bound-bound transitions, and not as resonant transitions into quasi-bound autoionizing levels [4]. However, while resonances may explain larger broadening of observed features in the Sandia experiments, that would not countenance uniformly higher monochromatic opacity in the (e + ion) bound-free continuum compared to theoretical calculations [3]. Atomic codes for opacities such as the Opacity Project (OP [6]), ATOMIC, OPAS and SCO-RCG (references in [3]), typically employ a wave function representation with uncoupled excitation channels into the residual core ion. Hence the photoionized atom or ion wavefunction expansion is incomplete, which results in (i) neglect of interference among overlapping infinite Rydberg series of autoionizing resonances converging on to excited cores, and large photoexcitation-of-core (PEC) resonances with characteristic asymmetric profiles (e.g. [7]), and (ii) "jumps" that enhance the background cross sections at excitation threshold(s) belonging to levels of successively higher-n complexes. The present coupled channel calculations show such jumps and enhancements in the (e + *ion*) continua, and that *coupling of the photoionizing level and the residual ion system requires completeness in terms of converged background up to sufficiently high energies.* In this *Letter* we report such completeness in calculations for the coupled Fe XVII → (e + Fe XVIII) system using the Breit-Pauli R-Matrix (BPRM) methodology, and demonstrate the aforementioned enhancement up to convergence and relevance to opacity models. Our study focuses on Fe XVII which is the highest contributor to opacity in the range T ∼ 150-200 eV (11-15 Ry or $2 \times 10^{6.24-6.37}$K) and electron densities $N_e \sim 10^{21-23}$ cm^{-3}, though the ionization fractions of the three dominant ions Fe XVII , Fe XVIII and Fe XIX in local thermodynamic equilibrium (LTE) at the Z temperature 182 eV (13.4 Ry) are 0.19, 0.38 and 0.29 respectively [3, 4].

Monochromatic plasma opacity κ_ν largely depends on radiation absorption through bound-bound (bb) photoexcitation and bound-free (bf) photoionization as follows:

$$\kappa_\nu^{bb}(i \rightarrow j) = \frac{\pi e^2}{mc} N_i f_{ij} \phi_\nu; \quad \kappa_\nu^{bf} = N_i \sigma_{PI}(\nu) \qquad (1)$$

where f_{ij} is the oscillator strength, σ_{PI} is the photoionization cross section, N_i is the ion density, and ϕ_ν is a profile factor. While oscillator strengths are discrete,

the cross sections form a continuum replete with resonant and background features. The contribution of σ_{PI} to the opacity may be expressed as an effective oscillator strength integrated over a given energy range ΔE

$$< f >_{\Delta E} = \sum_{k}^{\infty} \int_{\epsilon=E_k}^{\infty} \frac{df_{ik}}{d\epsilon} d\epsilon, \qquad (2)$$

where $df_{ik}/d\epsilon$ represents the photoionization continua that are now discretized according to excitation into ion core levels k from an initial level i. This is a non-trivial extension. In principle, *all* possible bound levels of the core ion contributing to the total (resonant+background) bound-free continuum, or σ_{ik} from an initial bound level i into a final $(e + ion)$ continuum with reference to the excited core levels k of the residual ion, should be included until convergence and no further enhancement. Explicitly including successive core excitations in σ_{PI},

$$< f >_{\Delta E} = \frac{1}{4\pi\alpha a_o^2} \sum_{E_1(k)}^{E_{n'}} \int_{\epsilon \geq E_k}^{\infty} \sigma_{ik} d\epsilon_k, \qquad (3)$$

where E_1 denotes the ground state of the core ion and $E_{n'}$ the highest level included in the coupled-channel calculations. We calculated σ_{ik} in the close coupling (CC) approximation using the R-matrix method [4]. We consider all possible dipole allowed transitions, which are typically the dominant ones, into states formed by configurations with the outer electron in n=2, 3, 4 shells.

Fig. 1 shows the photo-coupled [Fe XVII -Fe XVIII] system with a schematic diagram of the energy level structure of the core Fe XVIII ion included in the current calculations. The OP photoionization calculations for Fe XVII included only the ground complex of Fe XVIII , a 2 LS term expansion $1s^2 2s^2 2p^5$ ($^2P^o$) and $1s^2 2s 2p^6$ (^1S) (abbreviated as 2CC) [5]. The OP and other opacities calculations include these excited configurations, and inter-channel couplings and resonance structures, perturbatively. But that, for example, does not account for asymmetric autoionization profiles or coupled core excitations affecting background opacity. In a previous work [4] we considered 30 LS terms or 60 coupled fine structure levels up to the $n = 3$ complex; we refer to it as 30CC. We carried out the present calculations with a considerably larger expansion of the basis set up to 99 LS terms or 99CC, corresponding to 218 fine structure levels up to $n = 4$. The size of the Hamiltonian to be diagonalized in R-Matrix calculations increases as the total number of channels, hence the present calculations are more than an order of magnitude larger than in [4]. We calculated photoionization cross sections for all 283 bound LS states of Fe XVII up to $n = 10$ and $l = 9$, corresponding to 454 fine structure levels obtained in the previous work [4]. The OP calculation [5] has a much smaller number, 181 bound LS terms. Without loss of generality, and to optimize computational resources, we restrict the detailed calculations to 99 LS-coupled terms rather than a 218-level fine structure expansion, and use a coarser energy mesh than [4] to demonstrate the importance of enhanced background cross sections with broad PEC resonances and high-n core excitations; lower resolution *per se* should not lead to significant inaccuracy.

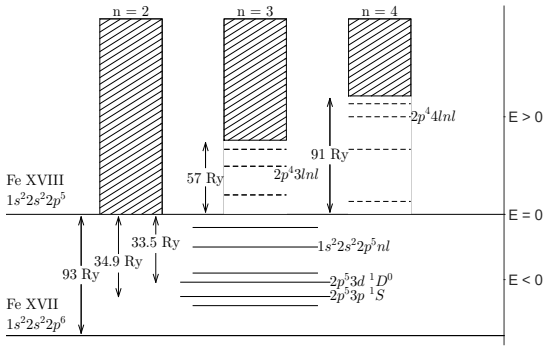

Figure 1: Schematic representation of (e + Fe XVIII) → Fe XVII bound and autoionizing levels included in the coupled channel calculations. The three results compared herein refer to calculations including 2 LS terms of $n = 2$ complex under the OP, previous 30 LS terms (60 fine structure levels) of $n = 2, 3$ [4], and the present 99 LS terms with $n = 2, 3, 4$ in the total wave function expansion. Illustrative results presented for photoionization in Fig. 3 of the 2 excited bound Fe XVII levels are highlighted (longer solid lines): $2p^5 3p\ ^1S$ and $2p^5 3d\ ^1D^o$.

Fig. 2 compares the σ_{PI} of the Fe XVII ground state from three different calculations and core excitations: (a) OP — 2CC, b) 30-CC, LS terms with $n \leq 3$ [4], and (c) the present 99-CC, LS terms with $n \leq 4$. Except for differing resolution of resonances, all three σ_{PI} have similar background cross sections; (b) and (c) are found to have small enhancements of 2% and 9% over the OP (a). Owing to fine structure splittings and higher resolution, the 30CC or 60-level cross sections (b), show more prominent resonances than the 99CC (c). In contrast to the ground state cross section, very large enhancements are found for excited state photoionization of Fe XVII , exemplified in Figs. 3, 4. Fig. 3a (top panel) show a detailed comparison of the OP monochromatic iron opacity with that measured at the highest temperature/ density achieved at the Sandia Z-machine, T = 2.11×10^6 K and $n_e = 3.1 \times 10^{22}$ *cc* [3]. The measured opacity spectra between 7-13Å corresponds to σ_{PI} in lower panels in the energy range ∼ 70 - 130 Ry. The prominent transition arrays in the measurement are due to three dominant Fe ionization states: Fe XVII , Fe XVIII and Fe XIX. The main points from the comparison are: (A) the measured background is consistently higher than OP throughout the energy range measured $7.5 \leq \lambda(\text{Å}) \leq 12.5$, (B) resonances are more broadened in experimental data, and (C) the "windows" in theoretical OP opacity in between resonance complexes appear to be filled in with higher background opacity.

Cross sections for the excited states $2s^2 2p^5 3p\ ^1S_0$ and $2s^2 2p^5 3d\ ^1D_2^o$ (Figs. 3b-c) are compared with the ob-

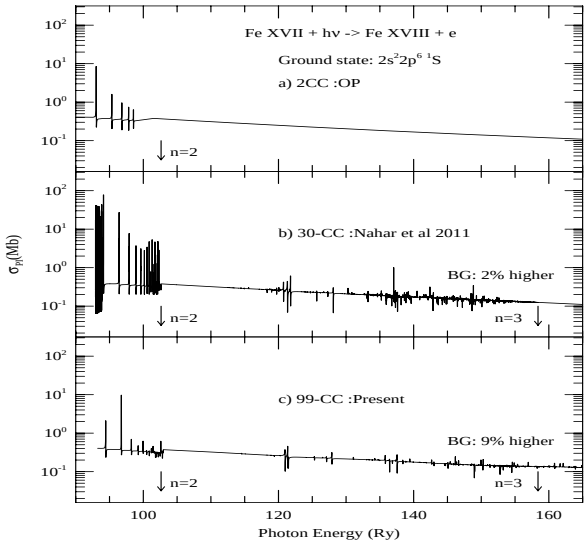

Figure 2: Comparison of photoionization cross sections σ_{PI} of the ground state of Fe XVII $2s^2 2p^6(^1S)$, using three different wave function expansions for the core ion Fe XVIII : (a) 2CC, the Opacity Project ([5], (b) 30CC (equivalent to 60 fine structure levels of [4]), and (c) the present 99CC. Arrows point to the highest thresholds for $n = 2$ and 3 excitations (the $n = 4$ thresholds up to 183.57 Ry are beyond the range shown). 'BG' is the background continuum at high energies; percentage enhancement relative to OP (a) is shown.

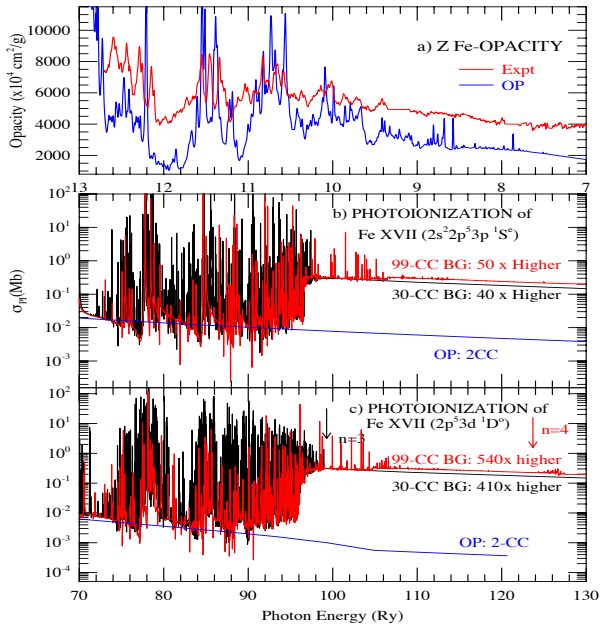

Figure 3: Comparison of σ_{PI} (panels b,c) of the excited $2s^2 2p^5 3p\ ^1S_0$ state of Fe XVII from the three sets of core excitations: 2CC OP [5] (blue curves), 30CC [4], and 99CC (present), with features in the opacity measurements at Sandia Z-pinch [3] (panel a). The energy range is the same, but in unit of Å for (a) and Ry for (b-c). Large enhancement factors relative to the OP (a) are marked.

served features in opacity (Figs. 3a). All three points (A,B,C) raised above can be accounted for by the present results. Most revealing is the enhancement of the background (BG) cross sections, which is much higher than OP throughout the high energy range by up to factors of 40 and 50 at the last continuum energy for the 30CC $n \leq 3$ and the 99CC $n \leq 4$ expansions respectively for the $\sigma_{PI}(2s^2 2p^5 3p\ ^1S_0)$ level (3b). An even larger background enhancement is seen for $\sigma_P I(2s^2 2p^5 3d\ ^1D^o)$, up to factors of 410 and 540 respectively compared to OP (3c). The enhancements are clearly related to the onset of the $n = 3$ and the $n = 4$ core excitation thresholds of Fe XVIII (c.f. Fig. 1). Furthermore, σ_{PI} decreases only marginally, even up to high energies, in the entire energy range corresponding to the Z-measurements (3a). To estimate the enhancement quantitatively, we calculated the averaged oscillator strength $< f >_{\Delta E}$ (Eq. 3) using the σ_{PI} (e.g. [7]) in the energy range of 70-130 Ry for the three states, the ground $2s^2 2p^6(^1S^e)$ and excited states $2s^2 2p^5 3p(^1S^e)$, $2s^2 2p^5 3d(^1D^o)$. The 2CC results with no excited n-complexes in the Fe XVIII expansion, underestimate the effective oscillator strength by up to two orders of magnitude (with the exception of the ground state); the $< f >$ values for the two excited states are 0.06, 1.81, 3.10 and 0.01, 1.86, 1.93 for 2CC, 30CC and 99CC calculations respectively. Including $n = 4$ core levels raises the *background* even below the $n = 3$ levels. Resonances grow weaker, leading to a smooth background at the highest $n = 4$ thresholds in Figs. 3b,c. Hence there is unlikely to be any significant enhancement by including higher $n > 4$ excitation thresholds (with far more cost), and the cross sections appear to have converged.

Another prominent feature is autoionizing resonances due to strong dipole PEC transition arrays (2p $\rightarrow$ 3s,3d) $n\ell$ and (2p $\rightarrow$ 4s,4d) $n\ell$ in the core ion Fe XVIII , with the spectator electron $n\ell$. Such PEC or Seaton resonances (e.g. [7]) remain large in photoionization of Rydberg levels with increasing n, even as the background decreases and σ_{PI} starts at lower ionization potentials. Fig. 4 shows a few of the computed σ_{PI} of the Rydberg series levels: $2s^2 2p^5(^2P^o)np\ ^3P$ with n = 3,4,5. Whereas, the background enhancement is large for $n = 3p$ and $n = 4p$, it is much smaller for $n = 5$, while the resonances at PEC positions are higher. Photoionization of Rydberg levels is often taken to decrease with energy as a power-law. But for L-shell ions while it is approximately true at high energies as one approaches the K-edge, [7], σ_{PI} remains substantial as in the present calculations (*viz.* Fig. 3). Even for σ_{PI} of a highly excited state $2s^2 2p^5 10p(^3P)$, the calculated $< f >$ is found to be much higher, 1.03, compared to 0.0013 from the OP cross sections. The energies of the strongest dipole transitions 2p $\rightarrow$ 3s,3d and 2p $\rightarrow$ 4s,4d arrays associated with the huge PEC

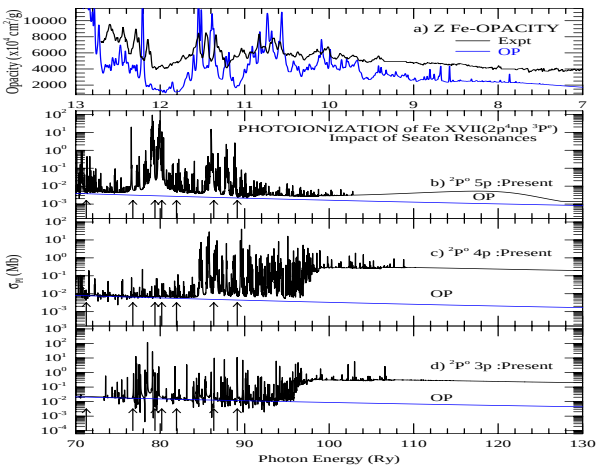

Figure 4: Comparison of features in the measured opacity spectrum [3] (a), with those due to PEC resonances in σ_{PI} of a series of Rydberg states $2s^2 2p^5 np(^2P^o)\ ^3P$ with n = 3, 4 and 5 (b-d). Transition energies corresponding to PEC resonances (not considered under OP [5]) are pointed out by arrows. The PECs are larger and wider resonances at higher excited states due to strong dipole core transitions that can enhance the background by orders of magnitude. The energy scale in panel (a) is in Å and in Ry in (b-d).

resonances are marked with arrows in the Fig. 4. These transition arrays correspond to the inverse process of dielectronic recombination via satellite lines (2p $\rightarrow$ ns,nd) $n'\ell'$, with the spectator electron $n'\ell'$. Interestingly, some of the PEC resonances in Fe XVII correspond to the energy region in between line (or resonant) features where the Z-opacity is much higher than the OP opacity (Fig-3a); including more ionization stages of Fe would further fill in the opacity.

Finally, we extend the atomic calculations to obtain monochromatic Fe XVII opacity at the Z plasma conditions shown in Fig. 5. The measured opacity (5a) is higher than the OP (5d), as is the present calculated opacity (5b,c). The considerable structure obtained in the present 99CC calculations (Fig. 5c) is mostly due to the large and broad PEC resonances, including autoionization broadening in an *ab initio* manner. We carry out a point-by-point normalized Lorentzian convolution over all 454 Fe XVII photoionization cross sections using an algorithm that simulates temperature-density dependent electron impact damping [12]. It is seen that most resonances dissolve into and raise the continuum opacity, filling in the windows in the OP data, as seen experimentally in 5a) [3]. That would also yield much greater *continuum lowering* than existing opacity calculations. The Rosseland Mean Opacity of Fe XVII from the present results is 170 cm^2/g, 35% higher than the 126 cm^2/g from OP. Substituting the present Fe XVII opacity alone into a solar mixture of all abundant elements from H to Ni, yields a 2.1% increase. However, Fe XVII is only one of the dominant ions under Z conditions with ionization fraction 0.195; Fe XVIII ionization fraction is 0.39, twice as much. Given the generality of the bound-free opacity enhancement shown in this *Letter*, including other contributing Fe ions such as Fe XVIII and Fe XIX , would be consistent with the 7% higher iron opacity from *all* iron ions in the Z data (perhaps higher), and consequently with the expected increase in total solar opacity that could solve the abundances problem. Furthermore, the current approach treats the structures and divisions between the bound-bound and bound-free opacities without unphysical approximations.

Opacity calculations involve several other important atomic-plasma issues. First, plasma broadening significantly affects the opacity distribution (c.f. Figs. 5b-c). Second, the Boltzmann factors in the equation-of-state (EOS) for Fe XVII imply low level populations in excited states, but there are nearly 200 such levels beginning 53 Ry above the ground state (Fig. 1) at the Z temperature $\sim 2 \times 10^6$K ($\exp(-\Delta E/k_B T) = 0.015$), and with fractional population between 0.1-1.0% of the ground state; augmented with orders of magnitude enhancement in cross sections that ensures a significant contribution to high-energy bound-free opacity. Third, the total oscillator strength sum-rule is sometimes invoked to rule out enhanced opacity as measured [13]. However, it is the *partial*, not the total, differential oscillator strength $\frac{df}{d\epsilon}$ in the relevant energy region, and atomic species at a given temperature-density, that determines the mean opacity. There would be substantial re-distribution of oscillator strength from the bound-bound, as in existing opacity models, to the bound-free once the atomic/plasma effects demonstrated herein are included. Fourth, the measured Fe ion fractions at the Z are close to LTE values [3]. Considering the multitude of high-n levels with large statistical weights [8], there are marked differences in occupation probabilities in the LTE EOS among different models [11]; sample calculations show that OP values from the Mihalas-Hummer-Däppen [9] EOS (also employed in this work) are *lower* than OPAL by 3% for $n = 3$, a factor of 6 for $n = 5$, and by 2 orders of magnitude for $n = 9$ [10]; therefore, an upward revision would further enhance the contribution of the present high-n σ_{PI} to opacity. The quantitative results presented herein help explain the observed discrepancies and the missing opacity due to photoabsorption from excited levels and core-excitations (the aforementioned points A, B and C). The present work also points to a basic feature of photoionization of any atomic system: the bound-free cross sections would be incomplete unless all contributing final states of the residual core ion are coupled. However, that greatly enlarges the scope of photoionization calculations even on state-of-the-art computational platforms. Generally, the enhancement and convergence of photoionization cross sections up to high energies should manifest itself in the bound-free plasma opacity of many astrophysical and laboratory sources (e.g. [14]).

We would like to thank Werner Eissner for contributions. This work was partially supported by the U.S.

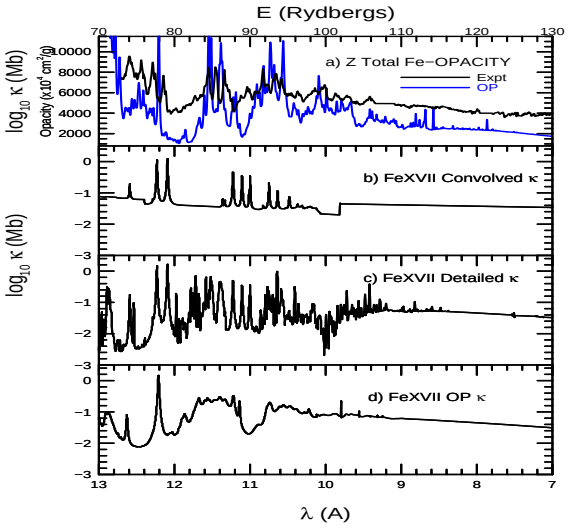

Figure 5: a): Total iron opacity measured at Z and OP at T = 2.1 $\times 10^6$ K and $n_e = 3.1 \times 10^{22}$ cm^{-3}. Present Fe XVII opacity b)-c): detailed autoionization resonance structures; c) convolved over electron impact broadening Lorentzian profile [12], which also fills in several windows in opacity compared to OP results d). Present values in b)-c) fall off more slowly than the OP d), and are higher in the high-energy region towards 7 Å.

Department of Energy (de-sc0012331) and and National Science Foundation (AST-1409207). The computational work was carried out at the Ohio Supercomputer Center in Columbus, Ohio.

∗ nahar.1@osu.edu, † pradhan.1@osu.edu

[1] M. Asplund, N. Grevesse, J. Sauval and P. Scott, Annu. Rev. Astro. Astrohys., 47, 481 (2009).

[2] J. Christensen-Dalsgaard, M. P. Di Mauro, G. Houdek, and F. Pijpers, *Astron. Astrophys.* , 494, 205 (2009).

[3] J. E. Bailey, T. Nagayama, G. P. Loisel, G. A. Rochau, C. Blancard, J. Colgan, Ph. Cosse, G. Faussurier, C. J. Fontes, F. Gilleron, I. Golovkin, S. B. Hansen, C. A. Iglesias, D. P. Kilcrease, J. J. McFarlane, R. C. Mancini, S. N. Nahar, C. Orban, J.-C. Pain, A. K. Pradhan, M. Sherill & B. G. Wilson, Nature, 517, 56-59 (2015). References to other radiation transport codes ATOMIC, OPAS, RCO-RCG, OPAL are given are given in this paper; some of them include more transition arrays than the OP, and the integrated mean opacities are similar.

[4] S. N. Nahar, A. K. Pradhan, G.-X. Chen & W. Eissner, *Phys. Rev. A* , 83, 053417 (2011).

[5] M. P. Scott; data at http: cdsweb.u-strasbg.fr/topbase/topbase.html

[6] M. J. Seaton, Y. Yu, D. Mihalas, and A. K. Pradhan, *Mon. Not. R. astr. Soc.* 266, 805 (1994); The Opacity Project Team, *The Opacity Project*, Institute of Physics Publishing, Vol 1, (1995); Vol. 2 (1996); OP opacities at http: opacities.osc.edu.

[7] A. K. Pradhan and S. N. Nahar, *Atomic Astrophysics and Spectroscopy*, Cambridge University Press (2011).

[8] J.-C. Pain and F. Gilleron, High Energy Density Physics, 15, 30-42 (2015).

[9] D. Mihalas, D. G. Hummer and W. Däppen, *Astrophys. J.* 331, 815 (1988).

[10] N. R. Badnell and M. J. Seaton, *J. Phys. B* , 36, 4367 (2003).

[11] R. Trampedach, W. Däppen and V. A. Baturin, *Astrophys. J.* , 646, 560-578 (2006).

[12] A new algorithm has been developed for numerical simulation of temperature-density dependent electron impact damping of autoionizing resonances in photoionization cross sections, tabulated at thousands of energies for each of the 454 bound Fe XVII levels. Point-by-point convolution with a Lorentzian functional is extremely CPU intensive, and would be described elsewhere.

[13] C. A. Iglesias, *High Energy Physics* , 15, 4 (2015).

[14] R. P. Drake, *High Energy Density Physics*, Springer (2006).